JME

Journal of Mining & Environment,
Vol.6, No.1, 2015, 1-10.

Geostatistical simulation of dyke systems in Sungun porphyry copper deposit, Iran

O. Asghari

Simulation and Data Processing Laboratory, School of Mining Engineering, University of Tehran, Tehran, Iran

Received 7 April 2013; received in revised form 20 June 2014; accepted 30 June 2014
Corresponding author: o.asghari@ut.ac.ir (O. Asghari).

Abstract
Post-mineralization activities may cause difficulties in the process of ore modeling in porphyry deposits. Sungun, NW Iran, is one of the porphyry copper deposits, in which dyke intrusions have made ore modeling more complicated than expected. Among different kinds of dykes, two types were chosen and the consequent geostatistical analyses were applied on. In this study, simple directional variograms were used for extracting relevant information from dyke systems on which the Sequential Indicator Simulations were applied consequently. One hundred realizations were produced on the simulation grid considering the anisotropy characteristics and E-type map has been provided averaging all realizations. Moreover, a binary state between dyke and non-dyke environments was produced putting threshold on the E-type grid node values to discriminate the ore from barren dykes. Hole-effect models were fitted to the empirical variograms perpendicular to the dyke strike. Dimensional information was elicited from these models and the results were compared with the previously carried out geological investigations, and finally a good numerical match was found between these two sources of information.

Keywords: *Dyke System, Variogram, Hole-Effect, Directional Features, SIS, Dimensional Features.*

1. Introduction

Post-mineralization phenomena usually make the modeling of geological phenomena a difficult procedure. This difficulty reaches its extremity in porphyry deposits mining when several barren dykes have intruded into ore deposit during several phases. They are often complicated structurally, which cannot be modeled easily and call for vast knowledge geology, dense data and a skilled expert to adopt the relevant methods in a logical order.

Dykes are sometimes barren and their proportion is not low enough to be overlooked. Furthermore, in any porphyry deposit, dykes cause problem in mining operations when they bear the potential to deteriorate the driller bit. One of the other important aspects of modeling dykes is the application of this model in the process of mining drainage. Such models can be obtained through simulation realizations since we deal with a global problem.

Geostatistics has opened a new era in the way through which one models the geological phenomena far better than previous methods, which were generally based on the layer cake models [1]. One of the most important steps of carrying out a geostatistical study is *structural analysis* [2].

Structural analysis tries to reflect the spatial variability of the regional variable [3]. One of the possible uses of indicator variogram is applied by Dubois to build ecological indicators to characterize and summarize spatio-temporal changes in the land cover on an annual basis [4]. There have been some well-done investigations in the field of remote sensing [5]. Woodcocka used variograms as a tool to identify models of ground scenes through spatial variation in remote sensing images. Jones and Ma related the geological characteristics of lithological bodies to experimental indicator variograms in a

comprehensive study in which the hole-effect models were the main tool of that study [6]. Also, they introduced the use of several multiplicative-composite variogram models to model hole-effect experimental variograms.
Sungun porphyry copper deposit, North-Western Iran, is studied where dyke intrusions have caused a lot of problems for mine engineers. Structural analysis is used as a powerful tool which to model dykes' main direction and dimensional features. Based on these features some models are provided and at the end the periodic nature of dykes in this deposit are investigated in more details.

2. Methodology

The model of alternating lithologies described by Jones and Ma is a realistic model, which can be found in operating mines and reservoirs abundantly [6]. Such dissimilarities measures can be used for further modeling steps, and confining variogram with the bounds of azimuth and dip would deliver useful information on the spatial continuity of the phenomenon under study in certain directions. "Omnidirectional" variogram calculation, which cannot be considered as an average of the various directional variograms, does not mean that the same spatial continuity can be found in all directions. The direction of maximum spatial continuity and the direction of minimum spatial continuity have been sought in every geostatistical research projects. Isaaks and Srivastava also mentioned the directional tolerance by which one can calculate the main axes of anisotropy [7].
In this study, at first, an overview of Sungun porphyry copper deposit is presented and the regional variable under study is illustrated and further geostatistical investigations are provided in detail:

3. Study area

Sungun porphyry copper deposit is located in Northwestern Iran (Azarbaijan province). Field observations and petrographic studies demonstrate that emplacement of the Sungun stock took place in several intrusive pulses, each with associated hydrothermal activity [8].

3.1. General geological settings

The host rock in Sungun deposit is a diorite/granodiorite to quartz monzonite stock [9,10]. The Sungun porphyry, occur as stocks and rarely in dykes and are series of calc-alkaline igneous rocks with a typical porphyritic texture [8]. Calagari detected four series of cross-cutting dykes varying in composition from quartz monzodiorite to granodiorite those are investigated in this research [11]. The deposit is sampled by a network of vertical, horizontal and dipping bore-holes with a regular density; on average each square $100m \times 100m$ contains one bore-hole (See Figure 1).

3.1.1. Dyke system

The dykes strike NNW-SSE, dip steeply to the west and have thickness from a few centimeters to several tens of meters (See Figure 1).
What is important and problematic is that the dykes appear to have acted as a barrier to hydrothermal and supergenes enrichment and consequently sometimes dilute the mills feed [12]. Table 1 shows the descriptive statistics of Cu grade in different rock units including dykes (DK1a, DK1b), and clearly, dykes are generally non-mineralized and is not worthy for the processing operations.
Among 41520 samples taken from Sungun, 29367 samples belong to Sungun Porphyries (70.7%), 7990 Samples belong to DK1a (19.2%) and 4163 samples belong to DK1b&c (10.1%). There are different kinds of dyke in Sungun among and DK1 is the most prevalent type which is mainly composed of Quartz Diorite to Quartz Monzonite. Three main types of dyke can be derived from DK1 known as DK1a, DK1b and DK1c, each of which has its own features [13] as follows: a) DK1a: This is the most prevalent type of dyke of type DK1. Those samples belong to DK1a have been exposed to a weak and medium to high degree of phyllic alteration. b) DK1b&c: On the other hand, samples show that DK1b is intruded before DK1a and has very weak phyllic and propylitic alterations. They don't bear any mineralization, and the amount of pyrite is very low. Besides, DK1c samples are in very weak propylitic alteration and sometimes they are intruded into the DK1b dykes. Figure 2 is a photo taken from a dyke that is highlighted by sub-vertical lines, and that bears distinct color helping geologists and miners to identify them.

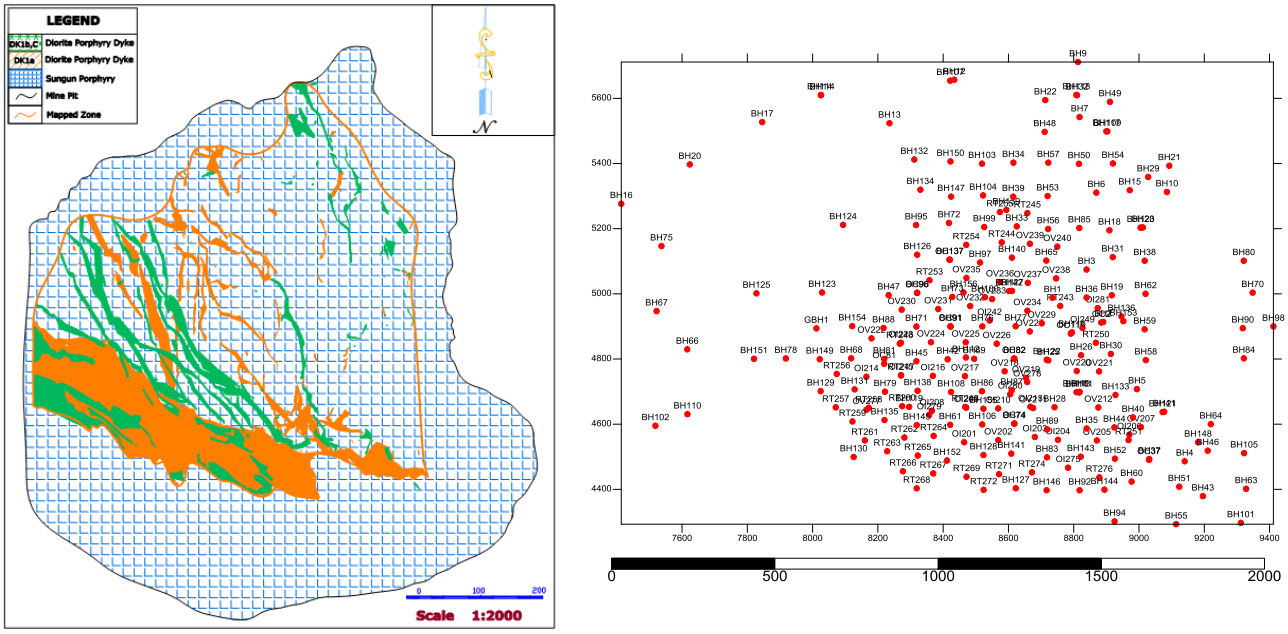

Figure 1. Dyke series are shown on a plan, and the selected area for this study is highlighted by orange line [13] (left) and Drill hole location plot, regular holes at the middle of area are drilled in the detailed exploration (right).

Table 1. Cu concentration statistical parameters in lithology units.

Rocktype	Mean (%)	Median (%)	Std. Deviation (%)
DK1a	0.076	0.013	0.19
DK1b	0.084	0.01	0.24
DK1c	0.039	0.01	0.14
SP	0.534	0.456	0.46

Figure 2. The change in color refers to dyke intrusion in Sungun Porphyry (northern 2300m bench, NW view).

4. Results and discussion

Further in this study, the processing steps done on the data are discussed:

4.1.Variography

Among grade and rocktype variables, an indicator state between dyke (DK1a and DK1b) and non-dyke environment has been focused on. The support of the variable is the core samples with length of L=2m. As DK1a and DK1b are the two main types of dyke in Sungun. The primary dataset is divided into two sets in each of which one of DK1a or DK1b (that itself includes DK1b, DK3 and DK1c) is 1 otherwise 0. The variography stage carried out on the datasets. These variograms include 22.5 degrees spaced

azimuthal and dip directions that sums up to 66 variograms considering one vertical and omnidirectional variogram.

Primarily, the omnidirectional variogram was drawn for DK1a indicator data, shown in Figure 3a. Hereafter, except for hole-effect models, all of the variograms fitted to experimental variograms are carried out using Schwanghart code that performs a least squares fit of various theoretical variograms to an experimental, isotropic variogram [14]. All variograms are fitted by a Spherical model. Isaaks and Srivastava explains why omnidirectional variogram can be useful for a geostatistical study [7]. At first, further directional calculations such as the lag distance and increment values can be optimized. Moreover, this variogram is useful when one plans to know how the overall structure of the data is, because the directional variograms may present erratic structure, and therefore hard to interpret. A trial and error procedure was followed to draw the most robust variogram structure that is shown in Figure 3. A discontinuity at 0-*nugget effect* $\gamma(h)$ does not seem to tend to zero when $h \to 0$ for this variogram, and this means that the regionalized variable is generally not continuous and is thus very irregular. "Geological noise" structures with a range shorter than the smallest inter-point distance and measurement or positioning errors all can be the reason for this phenomenon [3]. A *linear behavior* of the regionalized variable can be seen on the lags near the origin that means dykes are continuous, at least piecewise, but being no longer differentiable.

Omnidirectional variogram for DK1b is drawn and shown in Figure 3b where a strong spatial structure can be seen. Almost the same characters cannot be found for DK1b in terms of the dominant geometric anisotropy as the variation of sill and range does not differ a lot, but the behavior of omnidirectional variogram near the origin is the same as DK1a.

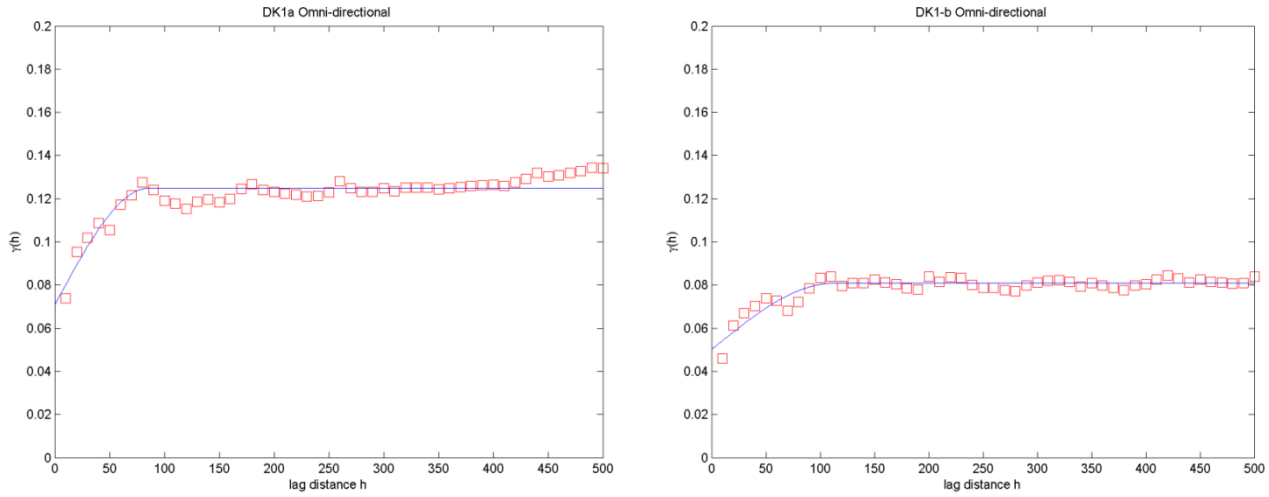

(a) **(b)**

Figure 3. DK1a omnidirectional variogram, g = 0.0707 + 0.0542 × Sph(86) (left) and omnidirectional variogram of DK1b g = 0.0501 + 0.0307 × Sph(112.33) (right).

Figure 4a shows the vertical and horizontal variograms introducing very structured variogram for vertical and variogram with more erratic features for horizontal direction. The regular fluctuation of the latter case is due to the relationship between the number of pairs and the semivariance. That is, more pairs for some lag distances coincide with more drill hole data samples and consequently higher variance values. Drill hole are generally spaced in 50 meters and the period of fluctuation on variogram can be related to this distance. The variogram in the direction perpendicular and parallel to DK1a strike and dip are drawn and held on (Figure 4b). For almost all lags, the variance depicted by the variogram perpendicular to dyke direction is higher than that of the other one.

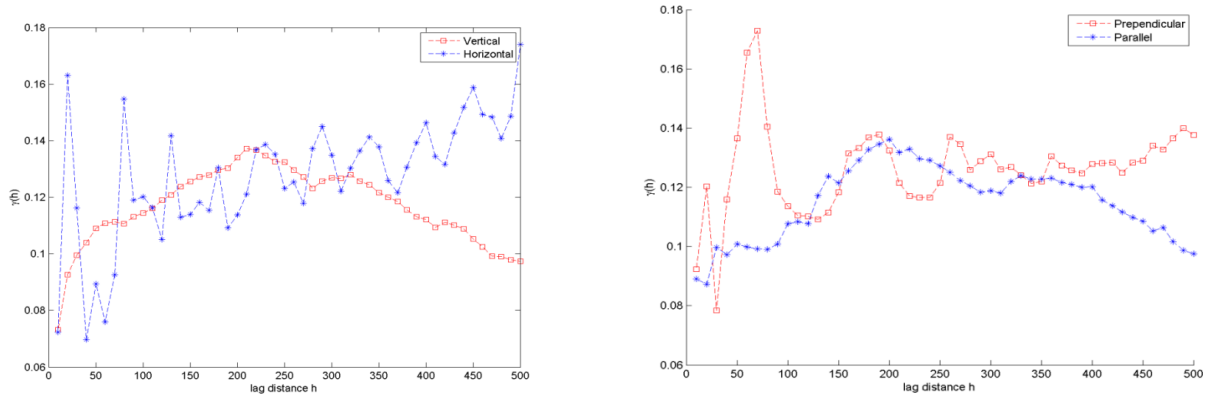

(a) **(b)**

Figure 4. Variograms in horizontal and vertical directions (left) and perpendicular and parallel to the dykes.

Moreover, since the dykes strike in certain and dominant direction, the variograms perpendicular and parallel to this strike may present more and less variances respectively. This relation can be used for identifying the orientation feature of the dykes.

Considering the fact that variograms can have larger continuities in the direction of strike of dyke, less variance and less nugget effect, the anisotropy directions were obtained for DK1a and DK1b and their features are brought in Table 2.

4.2. Hole- effect modeling

The presence of one or more bumps on the variogram corresponding to an equivalent number of holes on the covariance is the definition made by Chilès and Delfiner for Hole-effect, or it can be defined as a semi-variogram $\gamma(h)$ that display a hole-effect when its growth is not monotonic [15]. In Sungun, the same condition is found as the dyke occurrence is completely a periodic geological phenomenon. In this way, when the variogram model of this dyke is drawn, it is predictable to see hole-effect model.

Table 2. Anisotropy ellipsoid and the variogram characteristics of DK1a and DK1b.

DK1a	Azimuth	Dip	Range	Variogram Model
1	315	67.5	180	$\gamma = 0.078 + 0.047 \times Sph(180)$
2	135	22.5	78	$\gamma = 0.06 + 0.06 \times Sph(78)$
3	45	0	54	$\gamma = 0.13 \times Hole(61,210), Dampening = 210$
Sill	**0.0542**	**Nugget**	**0.0707**	
DK1b	**Azimuth**	**Dip**	**Range**	**Variogram Model**
1	337.5	67.5	224	$\gamma = 0.03 + 0.01 \times Sph(128) + 0.018 \times Sph(228)$
2	157.5	22.5	100	$\gamma = 0.02 + 0.03 \times Sph(100)$
3	67.5	0	68	$\gamma = 0.08 \times Hole(75,230), Dampening = 230$
Sill	**0.0307**	**Nugget**	**0.0501**	

In simple words, the direction in which the dyke is laid, there should be no or less strong hole-effect because it does not encounter any dyke when it searches for pairs. On the contrary, the most strong hole-effect model can be found perpendicular to the plane of the dyke.

Variograms with hole-effect can be divided into two main groups of without dampening and dampened models [16], and in the following section the two mentioned states are illustrated in Figure 5.

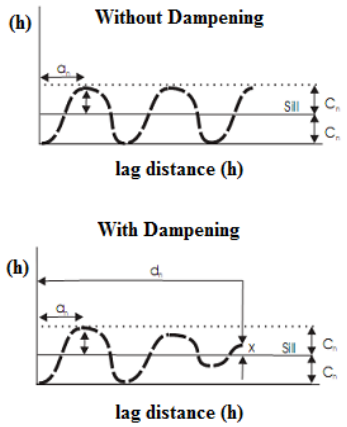

Figure 5. Parameters associated with the hole-effect model.

The main features of these two variograms are labeled on Figure 5, which are *sill*, *dampening distance* and *range*, but the hole-effect is usually dampened. This is caused by irregularities in feature intervals and by the superposition of other continuity structures. Dampening is achieved by multiplying the covariance function by an exponential covariance that acts as a dampening function and finally will be in the form of Equation 1:

$$\gamma = Sill \times \left(1 - e^{\frac{-S \times h}{d}} \times \cos(\frac{h \times \Pi}{range})\right) \quad (1)$$

The additional parameter d is the lag distance at which 95% of the hole-effect oscillation is dampened, named as *effective range* [17]. It should be noted that hereafter all Figures in which hole-effects are modeled having an X axis in radian scale, to compute the $\cos(\frac{h \times \Pi}{range})$ value.

4.2.1. Fitting a hole-effect model

An attempt is made to fit the best possible model with a hole-effect to the directional experimental semivariogram of DK1a and DK1b. The cosine model must be restricted to one dimension. This can be accomplished by setting the range parameters (ax, ay, az) to very large values in all directions except for the direction of the hole-effect structure [18]. Also, Journel and Huijbregts (1978) referred to the case when one wants to specify a particularly strong directional hole-effect, and mentioned that a positive definite hole-effect model in only one dimension must be used, like a cosine model.

As the nested structure of the hole-effect exist only in one direction, and the nested structure is limited to 1-D space, this makes the variogram dependent on only one component of the 3-D lag vector, h. Pyrcz and Deutsch discussed that this limitation is not significant, since most experimental hole-effect structures are only observed in one direction, like here since the hole-effect is seen only on the plane perpendicular to the dyke's plane [16].

First of all, DK1a's hole-effect was modeled using a cosine model and considering an exponential component to dampen the variogram shown in Figure 6. As can be seen, the first peak is fitted well; however, there is not such a well-fitted variogram to the experimental variogram thereafter. (The variogram model equation is provided below the Figures).

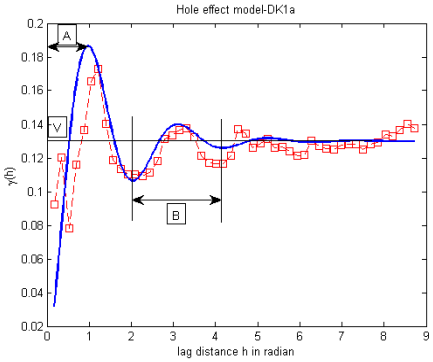

Figure 6. Hole-effect model and its wavelength fitted to the experimental variogram perpendicular for DK1a

$g = 0.13 \times Hole(61, 210), Dampening = 210$, units of range and dampening are in meter.

On the first place, the wavelength of this hole-effect model is calculated in two ways: from the hole-effect theoretical and experimental variogram. As it is shown in Figure 6, "A" is the distance to the first peak (0.5λ) which means that the wavelength is 112 meters [17]. Moreover, from the theoretical variogram it is about 61 meters and "B" value would be 122 meters. As Jones and Ma discussed, one can use the plateau V, (See Figure 6) in the quadratic equation $V = p(1-p)$ to obtain (Equation. 2):

$$\min(p, 1-p) = \frac{1 - \sqrt{(1-4V)}}{2} \quad (2)$$

where p and 1-p are the proportions of two facies (DK1a and Non-DK1a). As in the variogram in Figure 6, considering V value equals to 0.13 the p value could be computed, $P_{DK1\alpha} = 0.1536$ and consequently, P_{sp}=1-0.1536=0.8564.

It should be noted that SP refers to the non-DK1a environment; due to the name of Sungun Porphyry is labeled in SP, so it can contain other kind of rock types. These values are the exact values drawn from the primary drill holes data, 0.15and 0.85 for SP and DK1a respectively. The mean value of DK1a thickness can be computed too since we have the wavelength value of 122 and the $\mu_{SP} + \mu_{DK1\alpha} = \lambda = 122$

Where μ is the mean value of each facies. Now $\mu_{DK1\alpha}$ can be calculated as follows, $\mu_{DK1\alpha} = p \times \lambda = 18.3 \cong 18m$

The apparent range h* can now be obtained from the variogram in Figure 6 that is about 5.236 rad (300m) and considering the wavelength of 122 and referring to the plot (See Figure 7) provided by Jones and Ma one can obtain the point of apparent convergence to plateau, normalized to wavelength that is about 0.23. It should be noted

that in this plot we used the solid circles as they represent low or high facies fractions.

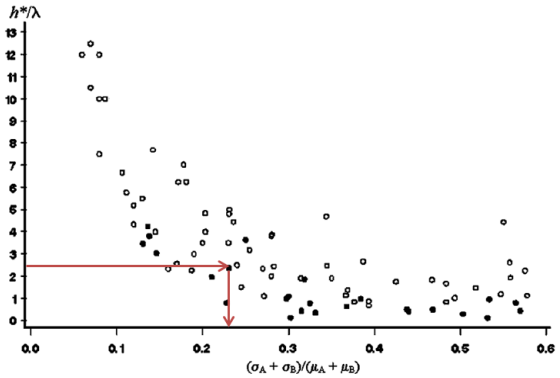

Figure 7. Crossplot of $\frac{h^*}{l}$ (point of apparent convergence to plateau, normalized to wavelength) vs. $(\sigma_A+\sigma_B)/(\mu_A+\mu_B)$. Open circles refer to moderate facies fractions $(0.3 \le p \ge 0.7)$ and solid circles refer to low or high facies fractions (Reprinted from Jones and Ma).

$$\frac{\sigma_{SP}+\sigma_{DK1\alpha}}{\mu_{SP}+\mu_{DK1\alpha}}=0.23$$

Where $\sigma_{SP}+\sigma_{DK1\alpha}$ is the total variation of thickness of the lithologic bodies, and in this way non-normalized total variation $(\sigma_{SP}+\sigma_{DK1\alpha})$ is 28.06 . The hole-effect model for DK1b is shown in Figure 8, and as can be seen just the first peak and tough are fitted well and the rest of experimental variogram does not follow the theoretical variogram well. The same procedure was followed for DK1b and using the parameters in Figure 8, the same information is calculated, but just the results are provided in this part:
All of the information on the dimensional features of DK1b is presented in Table 3.

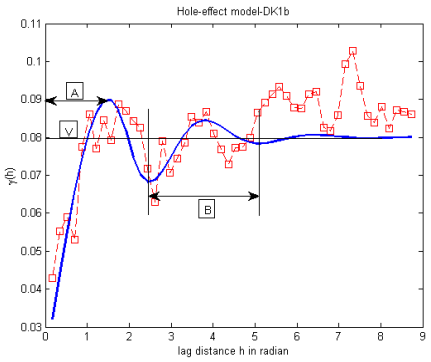

Figure 8. Hole-effect model fitted to the experimental variogram perpendicular for DK1a (left) $\gamma = 0.02 + 0.07 \times \text{Sph}(38.19)$, $\gamma = 0.08 \times \text{Hole}(75, 230)$. Dampening = 230 and the parameters used for getting the dimensional features of DK1b (right).

Table 3. Information calculated from dykes' hole-effect model.

Factor	Wavelength	V (Sill)	P(Proportion)	$\mu(Mean)$	$(\sigma_{SP}+\sigma_{DK1})$
DK1a	*122m*	0.13	0.1536	18m	28.06
DK1b	150m	0.08	0.087	13.15m	34.5

Geological information gathered through the past exploration and modeling phases are provided in Table 4, and it is clearly obvious that the results from hole-effect models are close to what the geologists have reached to over time.

Table 4. Information on dykes from geological prospecting for DK1a [13].

Geobody	Proportion	Width		Orientation	
DK1a	19 %	min	1.29	Azth	323
		mean	26.76	Dip	74.7
DK1b	7.4 %	min	1.71	Azth	8
		mean	17.23	Dip	69.1
		Max	86.69		

The dykes under study have been investigated geologically during the previously done projects, and the summary of this information is provided in Table 4, where the proportion, width and orientation features are presented for both dykes. In a comparison between what is calculated from the hole-effect models and directional variograms, and the geological data, a reasonable match can be found. At first, the proportion of dyke which is calculated from hole-effect models are 15 % and 8 % for DK1a and DK1b respectively, those are 19 % and 7.4 % for the DK1a and DK1b from geological investigations. Moreover, the mean value of dyke thickness is calculated from hole-effect model is 18 and 13.15 meters for DK1a and DK1b respectively, and the same parameters from geological investigations are 26.76 and 17.23 meters. Having the apparent (geological data) and real thickness (hole-effect models) of dyke, this difference can be justified. This can be found for

orientation features for dykes and except for the azimuth of DK1b other azimuth and dips are closely calculated from directional variograms.
Having done variography, Sequential Indicator Simulation (SIS) is used to model the dykes. A very short review of SIS is provided as follows.

4.3. Sequential Indicator Simulation

The limitations of Indicator Kriging moved geostatisticians at Stanford Center for Reservoir Forecasting (SCRF) forward to overcome inherent limitations that culminated in geostatistical simulations, Sequential Gaussian Simulation (SGS) and Sequential Indicator Simulation (SIS). The basis upon which these limitations have been obviated is the fact that simulation approach takes into account not only the spatial variation of observed data at sampled locations, but also the variation in estimations at unsampled locations, which kriging estimation ignores [18].

Chilès and Delfiner posed the question, "How Many Simulations Should We Generate?", and also refer to the objective and the structure of the phenomenon on which the study is carrying out [3]. A nonstationary field such as a petroleum reservoir or mine domain are the cases in which a single simulation provides a single answer because these are global problems. It is, therefore, necessary to build several simulations if we want to assess the range of the possible results. They believe that typically one hundred simulations may be needed. One hundred realizations were produced on a same grid and the E-type map was calculated by averaging all values (codes) for every single node. Figure 9a shows the E-type map for DK1a, in which the dyke-like structures, in terms of anisotropies, are reproduced to some extent.

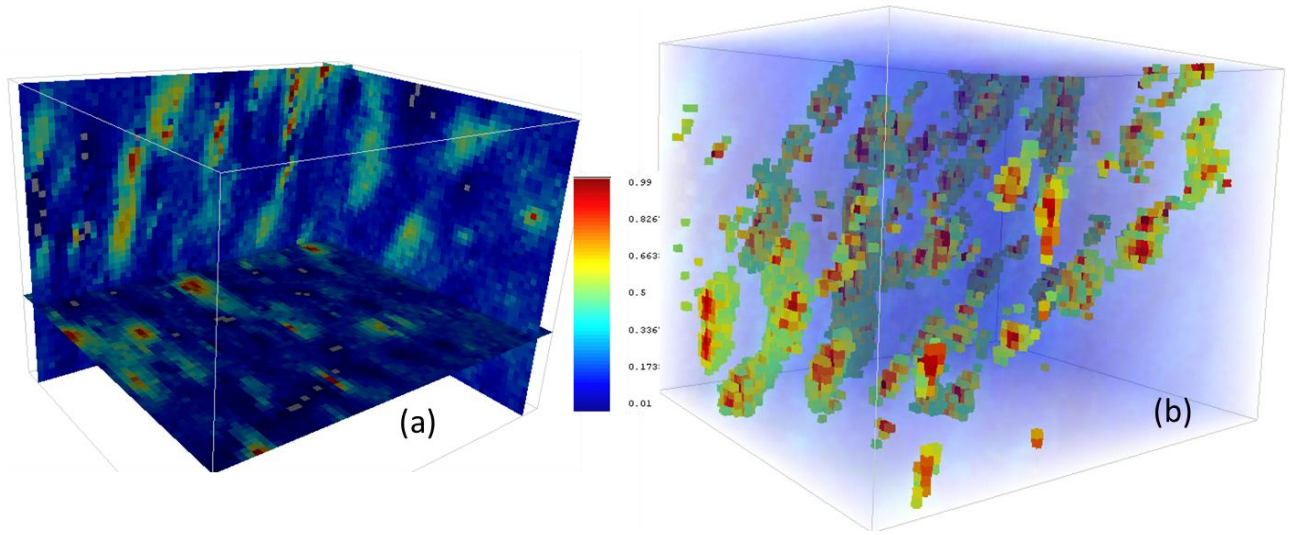

Figure 9. E-type grid for DK1a using SIS algorithm (a) and the binary state between dyke and non-dyke is represented considering 0.5 as the threshold of probability for DK1a (b).

E-type values are changed into an indicator state considering the cutoff value of 0.5; values more than 0.5 are changed into 1 and 0 for the values lower than cutoff. The final grid is shown in Figure 9b. As can be seen DK1a is simulated realistically, and they bear the same features like what is stated in the geological context of Sungun. The global proportion of DK1a reproduced from the simulation is 0.047 that is not equal to the proportion in the conditioning hard data which is 0.19. This can be due to the smoothing effect when one averages all realizations' values.
The same procedure was followed for DK1b, and the only difference is about the proportion of DK1b and its anisotropy ellipsoid. Consequently, the variogram model used for the simulation of DK1b differs. Figure 10a shows the E-type map for DK1b in which the higher values of probability are colored in red colors.
The same indicator state is prepared for DK1b. As it is shown in Figure 10b, the dyke structures are reproduced well and in the areas with more proportions of DK1b on hard data, thicker dykes are simulated.
Finally, all of simulation outputs are held on and they can be seen in one gird and view that may ease the process of comparison (See Figure 11).

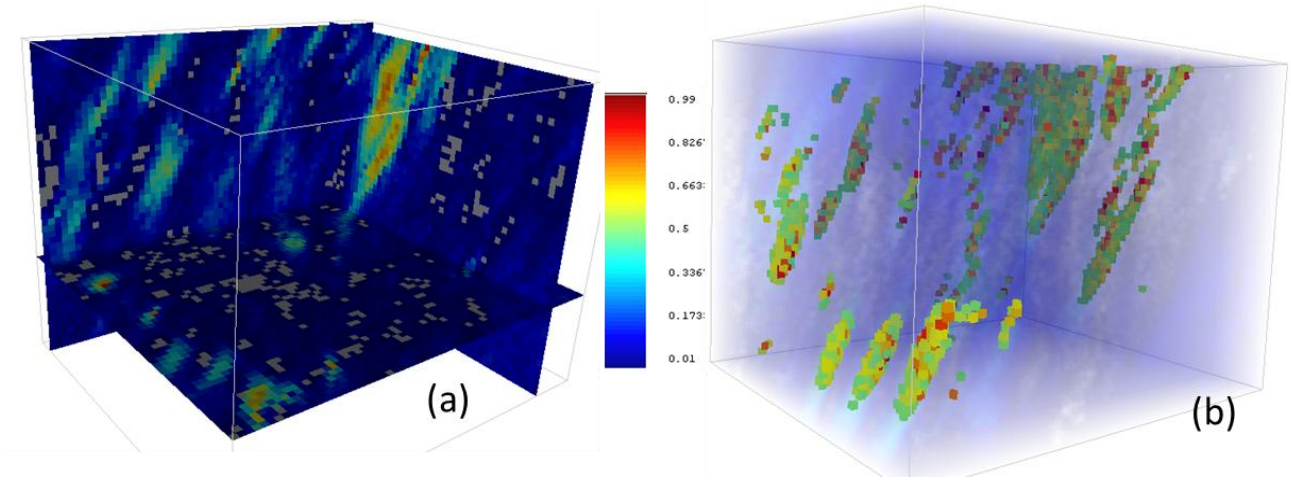

Figure 10. (a)E-type grid for DK1b using SIS and (b) the binary state between dyke and non-dyke is represented considering 0.5 as the threshold of probability for DK1b.

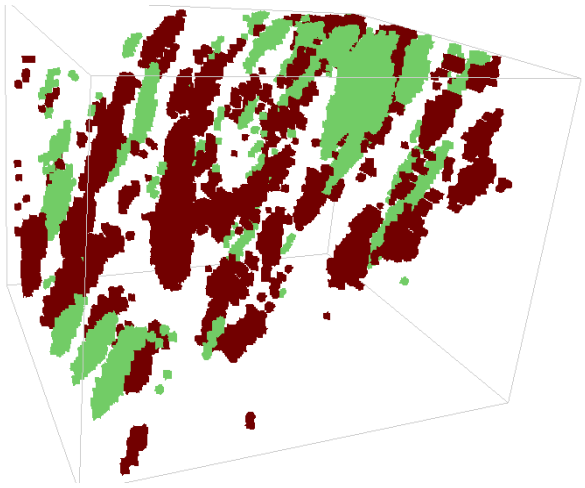

Figure 11. DK1a and DK1b simulation outputs in one grid (Red: DK1a, Green: DK1b).

5. Conclusions

A simplistic procedure is followed to get the orientation features of dykes under study using directional variograms. These features are used for modeling dykes using SIS that were applied on both kinds of dyke considered for this study. Realistic dyke-like structures were reproduced using SIS. Hole-effect models are useful tools in getting dimensional features of periodic phenomenon. Their applicability was proved when the results were compared with what we have in the geological investigations of Sungun's dykes. The only thing it needs is to identify the main axes of anisotropy and then draw and fit the empirical and theoretical models. To get more realistic results, what can be done in future is to consider the hole-effect models by which one can reproduce the periodic geological phenomenon like dyke systems. The models provided for dyke system can be used for mine planning of Sungun, where dykes cause problems in further mineral processing stages.

Acknowledgments

I would like to express my gratitude to Mr. Hassan Rezaee, my student at University of Tehran, for his worthy contribution to this research. I have to add that, modestly, he did not accept to be one of the authors of the manuscript. And also I would like to thank the Sungun Copper Mine authorities and especially P. Eng. Sharifi manager of the Sungun complex and Mr. Golchin, competent geologist, for providing us with comprehensive data for this study, and we are equally grateful to Parsolang Engineering Consultant Company for supporting this project with the needed geological data.

References

[1]. Matheron, G. (1971). The Theory of Regionalized Variables and its Applications. Les Cahiers du Centre de Morphologie Mathématique, Fasc. 5.

[2]. Journel, A.G. and Huijbregts, C.J. (1978). Mining Geostatistics. Academic Press, New York.

[3]. Chilès, J.P. and Delfiner, P. (1999). Geostatistics: Modeling Spatial Uncertainty, Wiley, New York.

[4]. Dubois, G. (2009). On the possible use of indicator variograms for building ecological indicators, In: Proceedings of the 33rd International Symposium on Remote Sensing of Environment (ISRSE), May 4-8, Stresa, Italy.

[5]. Woodcocka, C.E., Alan, S.H. and Juppc, D.L.B. (1988). The use of variograms in remote sensing: I. Scene models and simulated images, Remote Sensing of Environment. 25 (3): 323-348.

[6]. Jones, T.A. and Ma, Y.Z. (2001). Geologic characteristics of hole-effect variograms calculated from lithology-indicator variables: Mathematical Geology. 33 (5): 615–629.

[7]. Isaaks, E. and Srivastava, R. (1989). An Introduction to Applied Geostatistics, Oxford University Press, New York.

[8]. Hezarkhani, A. and Williams-Jones, A.E. (1998). Controls of alteration and mineralization in the Sungun porphyry copper deposit, Iran: Evidence from fluid inclusions and stable isotopes. Economic Geology. 93: 651-670.

[9]. Mehrpartou, M. (1993). Contributions to the geology, geochemistry, Ore genesis and fluid inclusion investigations on Sungun Cu-Mo porphyry de- posit, northwest of Iran. Unpublished PhD Thesis. University of Hamburg, Germany, 245 p.

[10]. Hezarkhani, A., Williams-Jones, A.E. and Gammons, C.H. (1999). Title of subordinate document. In: Factors controlling copper solubility and chalcopyrite deposition in the Sungun porphyry copper deposit, Iran. Mineralium deposita, 34: 770-783.

[11]. Calagari, A.A. (1997). Geochemical, stable isotope, noble gas, and fluid inclusion studies of mineralization and alteration at Sungun porphyry copper deposit, East Azarbaidjan, Iran: Implication for genesis. Ph.D. thesis, Manchester University, Manchester, 537 p.

[12]. Rashidinejad, F., Osanloo, M. and Rezai, B. (2008). Cut of Grades Optimization with Environmental management; a case study: Sungun Copper Porphyry Project, IUST International Journal of Engineering Science. 19 (5): 1-13.

[13]. Parsolang Engineering Consultant. (2006). Company Parsolang Modeling and Reserve Estimation Report of Sungun Copper Mine, Tehran.

[14]. Schwanghart, W. (2010). MATLAB Functions for GIS, Physical Geography, Hydrology, University of Basel, Department of Environmental Sciences, Physical Geography and Environmental Change.

[15]. Le, N.D. and Zidek, J.V. (2006). Statistical Analysis of Environmental Space-time processes. Springer.

[16]. Pyrcz, M.J. and Deutsch, C.V. (2001). The Whole Story of the Hole-effect, Centre for Computational Geostatistics 3rd Annual Report, Centre for Computational Geostatistics, University of Alberta, Canada.

[17]. Ma, Y. Z. and Jones, A.T. (2001). Teacher's Aide Modeling Hole-Effect Variograms of Lithology-Indicator Variables, Mathematical Geology. 33 (5).

[18]. Deutsch, C.V. and Journel, A.G. (1998). GSLIB: Geostatistical Software Library and User's Guide. 2nd edition, Oxford University Press, New York.

شبیه‌سازی زمین‌آماری سیستم دایک‌ها در کانسار مس پورفیری سونگون، ایران

امید اصغری

آزمایشگاه شبیه‌سازی و پردازش داده، دانشکده مهندسی معدن دانشگاه تهران، ایران

ارسال ۲۰۱۳/۴/۷، پذیرش ۲۰۱۴/۶/۳۰

نویسنده مسئول مکاتبات: o.asghari@ut.ac.ir

چکیده:

فعالیت‌های پس از کانی‌سازی ازجمله دایک‌های قطع کننده کانی‌سازی، مشکلاتی را در مدل‌سازی کانسار و به‌طور خاص کانسارهای پورفیری ایجاد می‌کند. در کانسار مس پورفیری سونگون واقع در شمال غرب ایران، تزریق این دایک‌ها باعث پیچیده شدن مدل‌سازی عیار شده است. در این پژوهش، از میان دایک‌های شناسایی شده، مطالعات زمین‌آماری مشتمل بر واریوگرافی جهت‌دار و شبیه‌سازی متوالی شاخص بر روی دو سری از آن‌ها صورت گرفت. بر اساس ناهمسانگردی شناسایی شده، یک‌صد مرتبه شبیه‌سازی صورت گرفت و نقشه میانگین آن‌ها نیز حاصل شد. بر روی نقشه میانگین و بر اساس آستانه تعریف‌شده، محیط کانسار به دایک و غیر دایک تفکیک شد. همچنین بر روی واریوگرام‌های تجربی در راستای عمود بر امتداد عمومی دایک‌ها، مدل اثر حفره (سینوسی) برازش شد. بر اساس نتایج مدل واریوگرام اثر حفره، اطلاعات مربوط به ضخامت دایک‌ها استخراج شد و نتایج با واقعیت انطباق داده شد.

کلمات کلیدی: سیستم دایک، واریوگرام، اثر حفره، ویژگی‌های جهت‌دار، شبیه‌سازی متوالی شاخص، ویژگی‌های واجد بعد.